Five-Coordinate Silicon in High-Silica Zeolites

H. Koller,*,† A. Wölker,† L. A. Villaescusa,‡ M. J. Díaz-Cabañas,‡ S. Valencia,‡ and M. A. Camblor‡

Contribution from the Institute of Physical Chemistry, University of Münster, 48149 Münster, Germany, and Instituto de Tecnologia Quimica, Universidad Politecnica, 46022 Valencia, Spain

Received November 23, 1998

Abstract: Pentacoordinated silicon units, $SiO_{4/2}F^-$, were found by solid-state NMR experiments in various as-made high-silica zeolites (Beta, SSZ-23, ITQ-3, ITQ-4, ZSM-12, Silicalite-1) that are prepared in the presence of fluoride ions as mineralizing agents. The $SiO_{4/2}F^-$ units are part of the framework, being connected, through sharing of the four O atoms, with four neighboring tetracoordinated $SiO_{4/2}$ units. These five-coordinate silicon units balance the charge of the cationic organic structure-directing agent. The ^{29}Si chemical shift of these sites is between −140 and −150 ppm, and the ^{19}F chemical shifts are between −56 and −78 ppm. The zeolites SSZ-23, ITQ-4, and Silicalite-1 show a dynamic motion of the fluoride ions at room temperature which is frozen out at a temperature of 130−140 K. In the case of fluoride motion, the ^{29}Si chemical shifts are between −120 and −150 ppm, indicating an exchange between four- and five-coordinate silicon, which means that the fluoride ions exchange between different framework silicon sites. The rigid $SiO_{4/2}F^-$ units show a characteristic parameter of the ^{19}F chemical shift anisotropy: the span value, $\Omega = \delta_{11} - \delta_{33}$, is between 80 and 87 ppm.

1. Introduction

The classical definition of zeolites is based upon their porous host structure that consists of fully connected $SiO_{4/2}$ and $AlO_{4/2}^-$ tetrahedra. Coordination numbers of silicon other than four are extremely rare in inorganic solids. Here, we show that this rule is violated for a whole class of zeolites: as-made high-silica zeolites that are prepared in fluoride medium using a cationic structure-directing agent (SDA) contain five-coordinate silicon in $SiO_{4/2}F^-$ units.

The silicon coordination number of four in zeolites seemed to be ubiquitous until a single-crystal X-ray structure of nonasil published by Van de Goor et al. established the first exception.[1] The crystals were prepared in fluoride medium using cobaltocenium ions ($Cocp_2^+$) as SDA. From here on we use the notation [Cocp₂]-F-[Si−NON], where the first bracket includes the guest species and the second bracket shows the framework constituents and topology, the latter being indicated by the three-letter code of the International Zeolite Association[2] for the nonasil (NON) structure.

The purposes of this paper are two-fold. The first is to show that $SiO_{4/2}F^-$ units are not just an unusual case that occurs only in nonasil, but rather are a general phenomenon found in high-silica zeolites that are synthesized by the fluoride method. The second purpose is to show that in some zeolites there is a dynamic motion of the fluoride ions which may be well characterized by ^{19}F and ^{29}Si solid-state NMR spectroscopy. The phenomena described in this work are fundamental for the understanding of the synthesis of (high-) silica zeolites under

Scheme 1
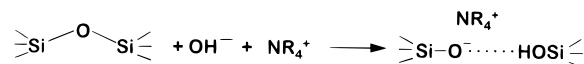
hydrothermal conditions using F^- as mineralizers, as they have implications on charge balance and on the phase selectivity.

High-silica zeolites are usually prepared under hydrothermal conditions, using a SiO_2 source, an SDA, a mineralizing agent, and water as the solvent. The SDA, which is occluded in the as-made zeolite, is most often a quaternary ammonium compound, and the mineralizing agent which is responsible for the hydrothermal reactivity of SiO_2 can be OH^- or F^- ions. A fundamental question regards the charge balance of the cationic SDA, since a three-dimensional, fully four-connected SiO_2 host would be neutral.

High-silica zeolites which are made in basic medium with OH^- ions as mineralizing agents have a substantial number of framework defects,[3] whereas zeolites are very poor in defect sites when the mineralizing species are F^- ions.[4] The formal equation (Scheme 1) illustrates the structural integration of OH^- ions in framework defect sites for the charge balance of quaternary ammonium cations in as-made high-silica zeolites. The hydrogen bonds between SiO^- groups and SiOH are identified by a very characteristic ^1H NMR line at ca. 10 ppm,[5] and to date they were found in about a dozen as-synthesized high-silica zeolites.

The recognition that fluoride ions can be used as mineralizing agents in zeolite synthesis was first reported in a patent by Flanigen and Patton,[6] and several groups have used this method in the past to make zeolites with a low defect site concentra-

* Corresponding author. Tel.: +49 251 832 3448. Fax: +49 251 832 9159. E-mail: hkoller@uni-muenster.de.
† University of Münster.
‡ Universidad Politecnica.

(1) Van de Goor, G.; Freyhardt, C. C.; Behrens, P. *Z. Anorg. Allg. Chem.* **1995**, *621*, 311.
(2) Meier, W. M.; Olson, D. H.; Bärlocher, C. *Atlas of Zeolite Structure Types*; Elsevier: New York, 1996; http://www.iza.ethz.ch/IZA-SC/Atlas/AtlasHome.html.
(3) Lobo, R. L.; Zones, S. I.; Davis, M. E. *J. Incl. Phenom. Mol. Recogn. Chem.* **1995**, *21*, 47.
(4) Chézeau, J. M.; Delmotte, L.; Guth, J. L.; Soulard, M. *Zeolites* **1989**, *9*, 78.
(5) Koller, H.; Lobo, R. F.; Burkett, S. L.; Davis, M. E. *J. Phys. Chem.* **1995**, *99*, 12588.
(6) Flanigen, E. M.; Patton, R. L. U.S. Patent 4073865, 1978.

Table 1. Synthesis Conditions and Chemical Composition of the Pure-Silica Phases

		synthesis conditions				phase composition
material[a]	zeolite name	crystallization mixture[b]	temp (K)	time (days)	ref	per unit cell[c]
[TPA]-F-[Si-MFI]	Silicalite-1	SiO_2: 0.08 TPABr: 0.4 NH_4F: 20 H_2O	448	7	4	$[C_{12}H_{28}N]_4F_4[SiO_2]_{96}$[d]
[TEA]-F-[Si-*BEA]	Beta	SiO_2: 0.54 TEAOH: 0.54 HF: 7.25 H_2O	413	1.6	8	$[C_8H_{20}N]_{5.7}F_5[SiO_2]_{64}$
[TMAda]-F-[Si-STT]	SSZ-23	SiO_2: 0.50 TMAdaOH: 0.50 HF: 15 H_2O	423	30	11	$[C_{13}H_{24}N]_{4.1}F_{3.3}[SiO_2]_{64}$
[DMABO]-F-[Si-ITE]	ITQ-3	SiO_2: 0.50 DMABOOH: 0.50 HF: 7.7 H_2O	423	28	9	$[C_{12}H_{24}N]_{3.9}F_{3.7}[SiO_2]_{64}$
[BQ]-F-[Si-IFR]	ITQ-4	SiO_2: 0.50 BQOH: 0.50 NH_4F: 14 H_2O	423	13	32	$[C_{14}H_{20}N]_{2.0}F_{1.8}[SiO_2]_{32}$
[M$_8$BQ]-F-[Si-MTW]	ZSM-12	SiO_2: 0.25 $M_8BQ(OH)_2$: 0.50 HF: 15 H_2O	448	14	this work	$[C_{22}H_{42}N_2]_{1.2}F_{2.4}[SiO_2]_{56}$

[a] Structure codes assigned by the International Zeolite Association. Zeolite Beta is a disordered, intergrown structure which is indicated by the asterisk (see ref 2 and http://www.iza.ethz.ch/IZA-SC/Atlas/STC.html). [b] SDA cations are denoted by their short names; see Scheme 2. [c] Experimental phase composition determined by chemical analysis of the guest species. No corrections have been made to account for small imbalances between the contents of charged SDA and fluoride. Thus, some formulas are not neutral, probably indicating the presence of small concentrations of defects of connectivity in the SiO_2 host. [d] Chemical analysis from reference.[36]

tion.[7–11] In addition, fluoride ions have also been used to synthesize aluminophosphates, gallophosphates, and other materials with zeolite-like porosity.[12–14] This paper is restricted to pure-silica zeolites.

The charge of the SDA in the aforementioned example, [Cocp$_2$]-F-[Si−NON], is balanced by the five-coordinate silicon units, $SiO_{4/2}F^-$. Our preliminary solid-state NMR work, which was published in a short communication, was carried out on [Cocp$_2$]-F-[Si−NON] and Silicalite-1 made with tetrapropylammonium cations, [TPA]-F-[Si-MFI].[15] The $SiO_{4/2}F^-$ groups in [Cocp$_2$]-F-[Si−NON] are characterized by a ^{29}Si NMR chemical shift of −145 ppm.[15] The fluoride ions in [TPA]-F-[Si-MFI] are mobile between different $SiO_{4/2}$ tetrahedra at room temperature, giving rise to an averaged [29]Si chemical shift of −125 ppm for silicon sites that change their coordination number between four ($SiO_{4/2}$) and five ($SiO_{4/2}F^-$). This fluoride motion can be frozen out at low temperature, which will be analyzed in more detail here.

Silicon atoms which are coordinated with five oxygen atoms have been reported for inorganic glasses and organic compounds.[16,17] Although the nucleophilic properties of the fluoride ions imply a driving force to form Si−F bonds, earlier results from X-ray diffraction on Silicalite-1[18] and octadecasil[19] did not give any indication on the formation of $SiO_{4/2}F^-$ groups. Especially the example with Silicalite-1 shows that X-ray diffraction may in some cases not be a straightforward method to track down the position of the fluoride ions. The motion of the fluoride ions at room temperature and the serious disorder of the structure-directing tetrapropylammonium cations, in addition to the problems in obtaining good single crystals (only twinned crystals or powdered samples were available so far), have prevented diffraction methods from locating the fluoride ions unambiguously. Two contradictory suggestions have been made based on X-ray diffraction,[18] but neither of them included the $SiO_{4/2}F^-$ units which are now established by solid-state NMR spectroscopy.[15] The clathrasil octadecasil has been thoroughly characterized by different NMR techniques, with special emphasis on the fluoride location.[20] These room-temperature data did not give any evidence for five-coordinate silicon in this structure. Thus, the question arises whether the zeolites [TPA]-F-[Si-MFI] and [Cocp$_2$]-F-[Si−NON] are two exceptional cases with five-coordinate silicon, or whether the double four-ring unit in octadecasil provides a special environment for fluoride ions that prevents them from binding to the zeolite framework.

The presence of pentacoordinated silicon can, in principle, be conveniently verified by ^{29}Si NMR spectroscopy. The chemical shift range of tetrahedral $SiO_{4/2}$ units in a high-silica environment is between −106 and −120 ppm.[21] Five-coordinate silicon in inorganic silicates has been observed between −145 and −150 ppm.[15,16] Cross-polarization from ^{19}F to [29]Si nuclei is a suitable method to increase the relative signal intensity of the $SiO_{4/2}F^-$ units due to the short Si−F distance. ^{19}F MAS NMR spectroscopy has been applied to high-silica zeolites,[14,19] and the isotropic chemical shifts were in the range of −38 to −173 ppm. This paper shows that ^{19}F NMR can be very informative if one goes beyond the determination of the isotropic chemical shift by analyzing the chemical shift anisotropy (CSA).

2. Experimental Section

Materials. All the materials except MTW were synthesized according to previously published procedures.[8–11] Table 1 lists synthesis conditions and chemical compositions of the final materials and Scheme 2 shows the organic cations used as SDAs. All the pure-silica zeolites used in this study were synthesized in fluoride medium at near-neutral pH (7.5–10.0). Silicalite-1 (MFI) was made at 448 K with NH_4F, Cabosil-M5, TPABr, and distilled water.[4] The other zeolites were synthesized by using tetraethyl orthosilicate, deionized water, HF (40%

(7) (a) Guth, J. L.; Kessler, H.; Caullet, P.; Hazm, J.; Merrouche, A.; Patarin, J. *Proceedings 9th International Zeolite Conference*; von Ballmoos, R., Higgins, J. B., Treacy, M. M. J., Eds., Montreal, 1992. (b) Deforth, U.; Unger, K. K.; Schüth, F. *Microporous Mater.* **1997**, *9*, 287. (c) Kuperman, A.; Nadimi, S.; Oliver, S.; Ozin, G. A.; Garcés, J. M.; Olken, M. M. *Nature* **1993**, *365*, 239. (d) Morris, R. E.; Weigel, S. J.; Henson, N. J.; Bull, L. M.; Janicke, M. T.; Chmelka, B. F.; Cheetham, A. K. *J. Am. Chem. Soc.* **1994**, *116*, 11849. (e) Lewis, J. E.; Freyhardt, C. C.; Davis, M. E. *J. Phys. Chem.* **1996**, *100*, 5039. (f) Lindlar, B.; Felsche, J.; Behrens, P.; Van de Goor, G. *J. Chem. Soc.* **1995**, 2559.

(8) Camblor, M. A.; Corma, A.; Valencia, S. *Chem. Commun.* **1996**, 2356.

(9) Camblor, M. A.; Corma, A.; Lightfoot, P.; Villaescusa, L. A.; Wright, P. A. *Angew. Chem.* **1997**, *109*, 2774.

(10) Barrett, P. A.; Camblor, M. A.; Corma, A.; Jones, R. H.; Villaescusa, L. A. *Chem. Mater.* **1997**, *9*, 1713.

(11) Camblor, M. A.; Díaz-Cabañas, M. J.; Perez-Pariente, J.; Teat, S. J.; Clegg, W.; Shannon, I. J.; Lightfoot, P.; Wright, P. A.; Morris, R. E. *Angew. Chem., Int. Ed.* **1998**, *37*, 2122.

(12) Estermann, M.; McCusker, L. B.; Bärlocher, C.; Merrouche, A.; Kessler, H. *Nature* **1991**, *352*, 320.

(13) Loiseau, T.; Taulelle, F.; Férey, G. *Microporous Mater.* **1997**, *9*, 83.

(14) Sierra, L.; Patarin, J.; Deroche, C.; Gies, H.; Guth, J. L. *Stud. Surf. Sci. Catal.* **1994**, *84*, 2237.

(15) Koller, H.; Wölker, A.; Eckert, H.; Panz, C.; Behrens, P. *Angew. Chem.* **1997**, *109*, 2939; *Angew. Chem., Int. Ed. Engl.* **1997**, *36*, 2823.

(16) Stebbins, J. F. *Nature* **1991**, *351*, 638.

(17) (a) Tacke, R.; Mühleisen, M.; Jones, P. G. *Angew. Chem., Int. Ed. Engl.* **1994**, *33*, 1186. (b) Holmes, R. R. *Chem. Rev.* **1990**, *90*, 17.

(18) (a) Price, G. D.; Pluth, J. J.; Smith, J. V.; Bennet, J. M.; Patton, R. L. *J. Am. Chem. Soc.* **1982**, *104*, 5971. (b) Mentzen, B. F.; Sacerdote-Peronnet, M.; Guth, J. L.; Kessler, H. *C. R. Acad. Sci. Paris Ser. II* **1991**, *313*, 177.

(19) Caullet, P.; Guth, J. L.; Hazm, J.; Lamblin, J. M.; Gies, H. *Eur. J. Solid State Inorg. Chem.* **1991**, *28*, 345.

(20) Fyfe, C. A.; Lewis, A. R.; Chézeau, J. M.; Grondey, H. *J. Am. Chem. Soc.* **1997**, *119*, 12210.

(21) Engelhardt, G.; Koller, H. *NMR Basic Principles Prog.* **1994**, *31*, 1.

Scheme 2

TPA   TEA   TMAda   DMABO

BQ   M$_8$BQ
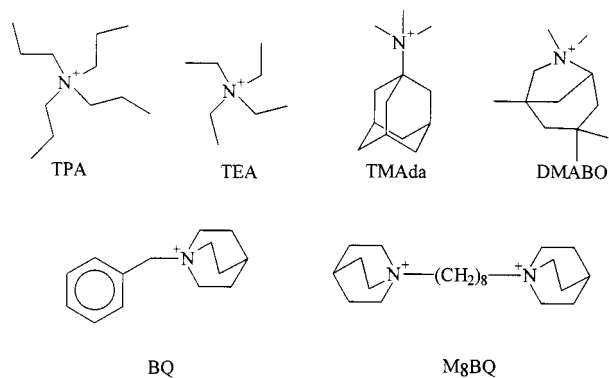
aqueous solution) or NH_4F, and the appropriate SDA in hydroxide form. When not commercially available, the SDAs were synthesized by quaternization of the parent amine by use of the appropriate halide. The halide obtained was then exchanged to the OH^- form by use of an ion-exchange resin. Tetraethyl orthosilicate was hydrolyzed in an aqueous solution of the SDA, and the mixture was stirred until complete evaporation of the ethanol produced (within the detection limit of ^{1}H NMR). Then, HF or NH_4F was added, and the mixture was stirred by hand or mechanically and transferred to Teflon-lined stainless steel autoclaves which were kept under rotation (60 rpm) for the required time.

Solid-State NMR. The ^{29}Si{^{1}H} CPMAS NMR spectra were recorded on a Bruker CXP-300 spectrometer which is upgraded with a Tecmag system, operating at a resonance frequency of 59.6 MHz. The [1]H $\pi/2$ pulse lengths range from 7 to 9 μs, the relaxation delays were either 5 or 10 s, and the contact time was typically 5, 10, or 15 ms. The samples were spun at 3–3.5 kHz in a zirconia rotor of 4 mm outer diameter. The data sampling lasted up to 12 h in order to achieve a good signal-to-noise ratio in these experiments. [29]Si{^{19}F} CPMAS and ^{19}F MAS NMR spectra were obtained on a Bruker CXP-200 spectrometer with a Tecmag system, using a double-resonance probe head with 7 mm rotors. The resonance frequencies were 39.8 MHz ([29]Si) and 188.3 MHz (^{19}F). The cross-polarization NMR spectra were not ^{19}F decoupled. The sample rotation was typically 3 kHz, but for ^{19}F MAS NMR spectra the spinning speed was also varied up to 6 kHz. The [19]F $\pi/2$ pulse lengths were between 9 and 12 μs. The Hartmann–Hahn match was optimized with Na_2SiF_6. The relaxation delays in these experiments were 20–30 s. Data accumulation in the ^{19}F MAS and ^{29}Si{^{19}F} CPMAS NMR spectra was as long as 12 and 26 h, respectively. The low-temperature experiments were recorded with conventional equipment from Bruker with cooling of the bearing gas. ^{19}F MAS NMR spectra were also recorded on a Bruker AMX-400 spectrometer, operating at a resonance frequency of 376.6 MHz.

3. Results

(a) ^{29}Si NMR. Figure 1 shows the ^{29}Si{^{1}H} CPMAS NMR spectra of the zeolites ITQ-4 (IFR), Silicalite-1 (MFI), SSZ-23 (STT), Beta (*BEA), ITQ-3 (ITE), and ZSM-12 (MTW). The ^{29}Si NMR signals of tetrahedral framework silicon are observed in the range from −98 to −117 ppm. ITQ-4 and SSZ-23 contain a small amount of Q^3 defect groups ($^-OSiO_{3/2}$ or $HOSiO_{3/2}$) as indicated by the signals at −99 (ITQ-4) and −100 ppm (SSZ-23). All zeolites have more than one crystallographic site for tetrahedral $SiO_{4/2}$ units, giving rise to multiple Q^4 lines.

The interesting part in the spectra regarding the presence of five-coordinate silicon between −115 and −150 ppm is magnified in the insets shown in Figure 1. The most obvious signals for five-coordinate silicon are observed in Figure 1b and e. Two sharp lines at −143.7 and −146.6 ppm for five-coordinate silicon are observed in Figure 1e (ITQ-3). The splitting of the two lines is due to *J* coupling with a coupling constant of about 180 Hz, as could be discerned by changing the magnetic field:
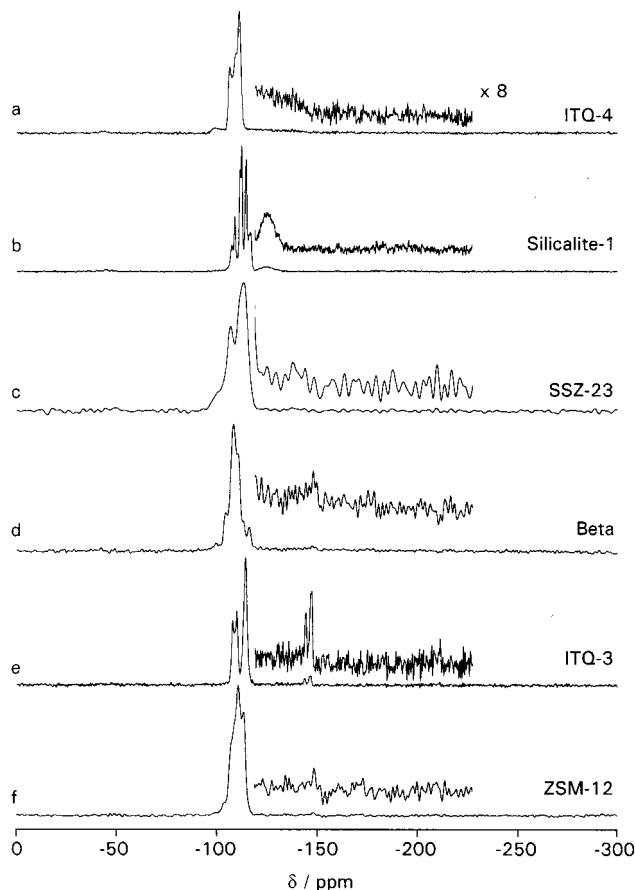

Figure 1. ^{29}Si{^{1}H} CPMAS NMR spectra of zeolites (a) ITQ-4 (IFR), (b) Silicalite-1 (MFI), (c) SSZ-23, (d) Beta (*BEA), (e) ITQ-3 (ITE), (f) ZSM-12 (MTW).

a ^{29}Si{^{1}H} CPMAS NMR spectrum at 39.7 MHz has the two signals at −142.8 and −147.4 ppm. It seems to be unusual that the intensities of the doublet are not the same, but similar results have, for example, been reported for ^{31}P NMR spectra on fluorophosphates,[22] where the Hamiltonian of internal spin interactions is dominated not only by spin–spin coupling, but also by heteronuclear dipole interaction and CSA. The effect described in ref 22 could be one reason we do not observe *J* coupling doublets for the $SiO_{4/2}F^-$ units in all zeolites. One line of the doublet could just be too weak and be obscured in the noise. ZSM-5 shows a broad line at −125 ppm at room temperature (Figure 1b). The spectrum of ITQ-4 shown in Figure 1a shows a very broad signal in the range between −115 and −140 ppm. Thus, the three zeolites ITQ-4, Silicalite-1, and ITQ-3 show ^{29}Si NMR signals in the range between −115 and −150 ppm, which are not due to four-coordinate $SiO_{4/2}$ units, but must originate from five-coordinate silicon sites. No clear proof for five-coordinate silicon can be ascertained in the ^{29}Si{^{1}H} CPMAS NMR experiments of SSZ-23, Beta, and ZSM-12 (Figure 1c,d,f). However, ^{29}Si MAS NMR spectra without cross-polarization of SSZ-23[11] and zeolite Beta show lines at ca. −138 and −147 ppm, respectively, which are due to five-coordinate silicon (not shown). These signals are obviously too weak in the ^{29}Si{^{1}H} CPMAS NMR spectra.

More information is obtained from the ^{29}Si{^{19}F} CPMAS NMR spectra shown in Figure 2. All signals in the range from −115 to −150 ppm for five-coordinate silicon are relatively enhanced by this technique as compared to Figure 1. In

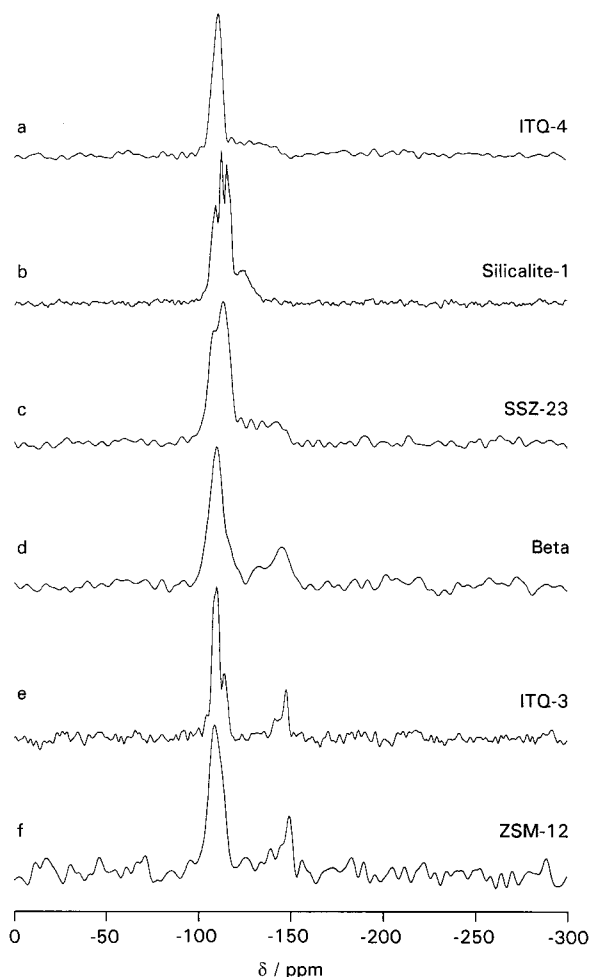(22) Haubenreisser, U.; Sternberg, U.; Grimmer, A.-R. *Mol. Phys.* **1987**, *60*, 151.

Figure 2. $^{29}Si\{^{19}F\}$ CPMAS NMR spectra of zeolites (a) ITQ-4 (IFR), (b) Silicalite-1 (MFI), (c) SSZ-23, (d) Beta (*BEA), (e) ITQ-3 (ITE), (f) ZSM-12 (MTW).

Figure 3. $^{29}Si\{^{19}F\}$ CPMAS NMR spectra of Silicalite-1 (MFI) with different contact times.

particular, a very broad signal can now be discerned at −120 to −150 ppm in Figure 2c for SSZ-23, and zeolite Beta shows a peak at −145 ppm in Figure 2d. Even the $^{29}Si\{^{19}F\}$ CPMAS NMR spectrum of ZSM-12 has a signal at −149.2 ppm for five-coordinate silicon. The enhancement of the ^{29}Si NMR signals for pentacoordinate silicon is due to the short Si−F distances in the $SiO_{4/2}F^-$ units, which facilitates cross-polarization between the two nuclei. Interestingly, some signals of four-coordinate silicon are also relatively enhanced in the $^{29}Si\{^{19}F\}$ CPMAS NMR spectra of Figure 2, such as the line at −107 ppm for SSZ-23 or the peak at −110 ppm for ITQ-3. These four-coordinate silicon atoms must be spatially close to the fluorine of the five-coordinate silicon units.

In what follows, a few characteristic ^{29}Si NMR properties of the five-coordinate silicon units will be discussed. The $^{29}Si\{^{19}F\}$ CPMAS NMR experiments are very time-consuming. This is due in part to the long relaxation delays (20−30 s) necessary to run these spectra, because the T_1 relaxation of ^{19}F is relevant here. In addition, the sensitivity of these experiments turned out to be low. The poor efficiency of the $^{29}Si\{^{19}F\}$ CPMAS NMR experiment for MFI at fast spinning rates has also been reported by Marcuccilli Hoffner et al.[23]

Figure 3 shows the $^{29}Si\{^{19}F\}$ CPMAS NMR spectra of MFI with varying contact times. Clearly, a difference in the cross-polarization dynamics can be discerned between four- and five-
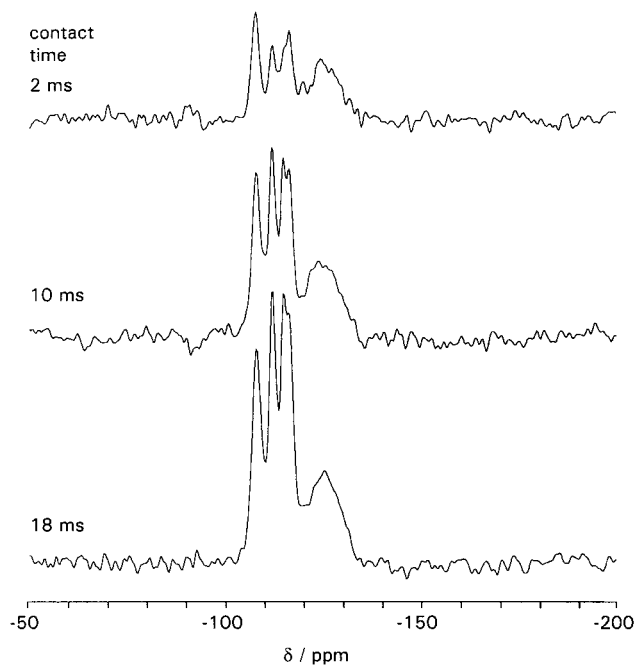
coordinate silicon. A relative increase in intensity is observed for the signals between −105 and −118 ppm with longer contact times, while the intensity of the broad signal at −125 ppm is much less sensitive to changes in the contact time. This observation proves that these latter sites are closest to fluorine, because their cross-polarization intensity is already relatively large at short contact times.

A second and unusual indication for the difference in the $^{19}F-^{29}Si$ heteronuclear dipole interaction between four- and five-coordinate silicon sites is obtained from experiments with and without ^{19}F decoupling. The signals for $SiO_{4/2}F^-$ sites are clearly visible, if the experiments are performed without ^{19}F decoupling (Figures 2 and 3). Surprisingly, the same experiments with ^{19}F decoupling (not shown) exhibit a substantial broadening for the signals originating from the $SiO_{4/2}F^-$ units, whereas the four-coordinate $SiO_{4/2}$ sites do not show this broadening. Although decoupling is meant to narrow all the lines, ^{19}F irradiation during data acquisition causes a selective broadening of the signals of the $SiO_{4/2}F^-$ units. Further work to study this unusual observation in more detail are ongoing, but the results are out of the scope of this paper. At the present stage, we consider two different mechanisms for this line broadening upon ^{19}F decoupling. The first possibility is that the large ^{19}F CSAs (see below) make the heteronuclear dipole interaction difficult to decouple by conventional radio frequency irradiation, especially when the coupling constants are large. Such effects have been described for proton decoupling in ^{13}C NMR where the protons have a large hyperfine coupling to paramagnetic centers.[24] The second possibility for this unusual decoupling behavior is a mechanism that has been described by Griffin and coauthors.[25] The effect has been called "rotary resonance recoupling", and it occurs when the decoupling rf field is a multiple of the rotor spinning frequency. Our rf field was 27 kHz, and the spinning speed was 3 kHz. We have attempted to change the experimental parameters to avoid the line broadening. However, unfortunately,

(23) Marcuccilli Hoffner, F.; Delmotte, L.; Kessler, H. *Zeolites* **1993**, *13*, 60.

(24) Clayton, A. N.; Dobson, C. M.; Grey, C. P. *J. Chem. Soc., Chem. Commun.* **1990**, 72.

(25) Oas, T. G.; Griffin, R. G.; Levitt, M. H. *J. Chem. Phys.* **1988**, *89*, 692.
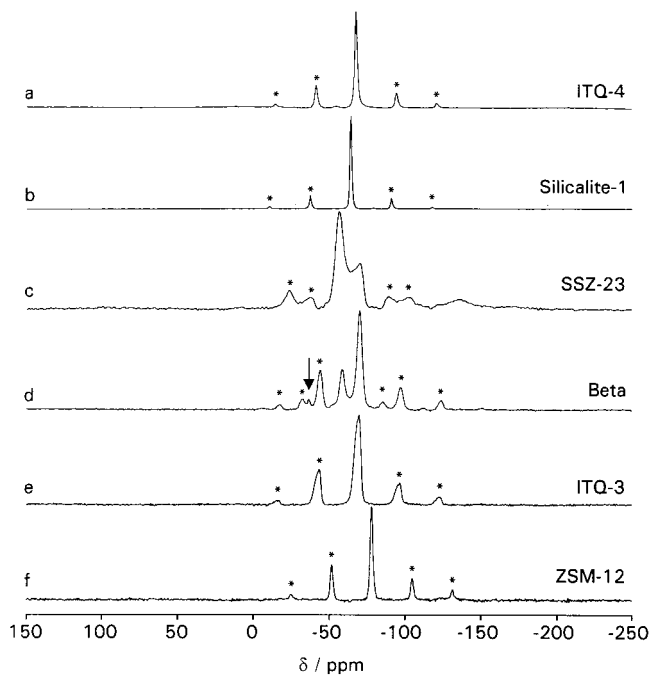
Figure 4. ^{19}F MAS NMR spectra of zeolites (a) ITQ-4 (IFR), (b) Silicalite-1 (MFI), (c) SSZ-23, (d) Beta (*BEA), (e) ITQ-3 (ITE), (f) ZSM-12 (MTW); spinning sidebands are marked with an asterisk, and a minor impurity in zeolite Beta is indicated by an arrow.

Figure 5. ^{19}F MAS NMR spectra of zeolite Beta (a, d) recorded at magnetic fields of 4.7 and 9.4 T along with simulated spectra (b, e) and individual components (c, f); spinning sidebands are marked with an asterisk, and a minor impurity is indicated by an arrow.

the experimental window for the rf power and spinning speed for a successful cross-polarization experiment was very narrow, and the broadening was unaffected by small changes in the conditions. The present system is unusual in that it has a strong heteronuclear dipole coupling of isolated two-spin pairs which seems to make the decoupling efficiency rather unique. ^{29}Si MAS NMR spectra without cross-polarization are not suitable to get strong enough signals of the $SiO_{4/2}F^-$ sites to study the decoupling in more detail.

For all samples, the ^{29}Si NMR signals of five-coordinate silicon units are in the range between -115 and -150 ppm. Zeolite Beta, ITQ-3, and ZSM-12 exhibit lines between -140 and -150 ppm, while ITQ-4, Silicalite-1, and SSZ-23 have broad signals in the range from -115 to -150 ppm. For Silicalite-1 it has been shown that the broad signal at -125 ppm is due to a dynamic average of 4- and 5-coordinate silicon, because the fluoride ions exchange between different silicon sites.[15]

(b) ^{19}F NMR. Further evidence regarding the incorporation and motion of fluoride ions in zeolites can be obtained from the ^{19}F NMR experiments shown in Figure 4. Zeolites Beta (-58.6 and -70.3 ppm) and SSZ-23 (-56.3 and -70.3 ppm) show two ^{19}F NMR signals for $SiO_{4/2}F^-$ groups, and ITQ-3 exhibits an asymmetric signal at -69.6 ppm. All other zeolites show only one isotropic fluorine resonance (IFR at -67.4 ppm, MFI at -64.0 ppm, MTW at -78.0 ppm). The spectra in Figure 4 show well-separated spinning sidebands. The absolute intensities of the ^{19}F NMR signals correlate well with fluorine elemental analysis. The concentration of fluoride ions in the zeolite samples is generally in good agreement (within 10%, see Table 1) with what is needed to balance the charge of the cationic SDAs. Thus it is concluded that the positive charge of the SDA is balanced by the $SiO_{4/2}F^-$ units in the zeolite framework found by ^{29}Si NMR (see above). Only SSZ-23 has a slightly lower concentration of fluoride ions than is needed for charge balance, which explains the presence of the afore-mentioned defect sites to provide the necessary concentration
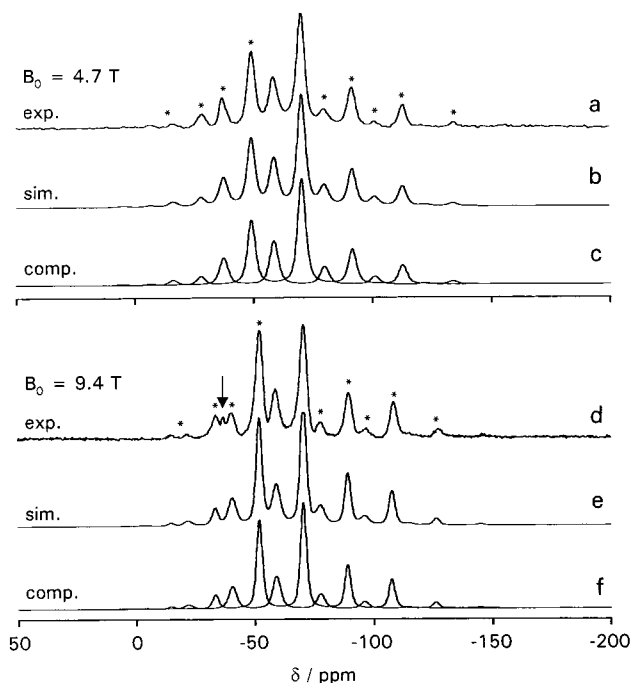
of anionic charge centers.[11] Accordingly, this sample shows a small signal at 10 ppm in the ^{1}H MAS NMR spectrum for the $SiO^-\cdots HOSi$ hydrogen bonds which are not found in the other zeolites.

The origin of the spinning sidebands in the ^{19}F MAS NMR spectra is the next question that is addressed. They can be due either to ^{19}F CSA or to homo- or heteronuclear dipole interactions. If the spinning sidebands are mainly caused by ^{19}F CSA, then they can be simulated according to the method introduced by Herzfeld and Berger.[26]

This spinning sideband analysis yields the principal components δ_{11}, δ_{22}, and δ_{33} of the anisotropic chemical shift tensor. From these components are derived the isotropic chemical shift, $\delta_{iso} = 1/3(\delta_{11} + \delta_{22} + \delta_{33})$; the span, $\Omega = \delta_{11} - \delta_{33}$; the asymmetry parameter, $\eta = (\delta_{22}-\delta_{11})/(\delta_{33}-\delta_{iso})$, and the skew, $\kappa = 3(\delta_{22}-\delta_{iso})/\Omega$.[27] To test whether homonuclear ([19]F$-$[19]F) or heteronuclear ([19]F$-$[1]H) dipole interactions contribute to the spinning sideband intensities, the ^{19}F MAS NMR experiments were measured at two different magnetic field strengths, i.e., at $B_0 = 4.7\ T$ and $B_0 = 9.4\ T$. The case of zeolite Beta shown in Figure 5 is one of the more difficult ones to analyze, because of the presence of two components, which makes it to a good test case for the reliability of the applied spinning sideband analysis. The figure shows the ^{19}F MAS NMR spectra of zeolite Beta at the two different magnetic fields (Figure 5a,d) along with the simulated spectra (Figure 5b,e) and components (Figure 5c,f). The two different ^{19}F NMR experiments (Figure 5a,d) were simulated with a single model that employs only CSA as the cause for the spinning sidebands. The consistent simulation at two magnetic fields proves that dipole interactions, homo- or heteronuclear, do not play a significant role, and the ^{19}F spinning sideband patterns are due to CSA. The same result has been obtained on all the other zeolite samples except SSZ-23. The obtained parameters are listed in Table 2. The estimated

(26) Herzfeld, J.; Berger, A. E. *J. Chem. Phys.* **1980**, *73*, 6021.
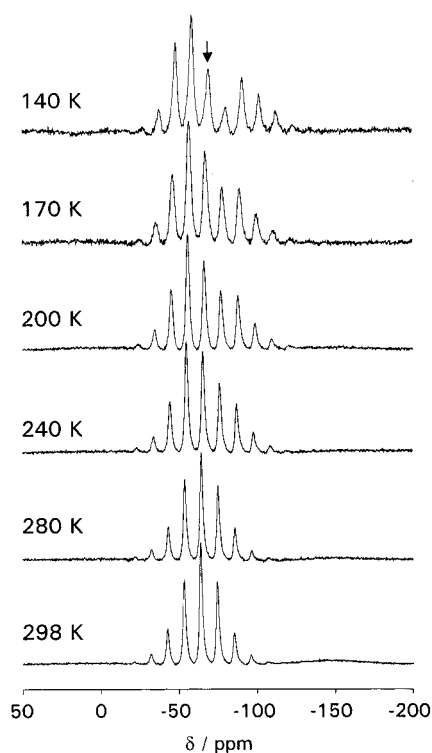(27) Mason, J. *Solid State NMR* **1993**, *2*, 285.

Table 2. ^{19}F NMR Data of Zeolites ITQ-3 (ITE), ITQ-4 (IFR), Silicalite-1 (MFI), SSZ-23 (STT), Beta (*BEA), and ZSM-12 (MTW)

	δ_{iso}/ ppm	δ_{11}/ ppm	δ_{22}/ ppm	δ_{33}/ ppm	Ω/ ppm	η	κ
ITQ-3	−69.1	−36.1	−53.4	−117.7	81.6	0.36	0.58
ITQ-4	−67.8	−37.5	−59.0	−106.9	69.4	0.55	0.38
Silicalite-1	−63.9	−37.8	−63.8	−90.1	52.3	0.99	0.01
SSZ-23	−56.4						
	−68.9						
Beta	−70.4	−37.1	−54.7	−119.3	82.2	0.36	0.57
	−59.0	−23.2	−49.9	−103.8	80.6	0.60	0.34
ZSM-12	−78.1	−44.3	−61.0	−129.0	84.7	0.33	0.61

confidence of the Ω values is 4 ppm or better. The ^{19}F MAS NMR spectrum of SSZ-23 could not be satisfactorily simulated at room temperature for the two different magnetic fields. Especially the less intense component, at −68.9 ppm, shows a large dependence of the spinning sidebands on the magnetic field. We interpret this by a motion of the fluoride ions on an intermediate NMR time scale which does not allow for the application of the method by Herzfeld and Berger.[26]

At this point a comparison between the ^{19}F and ^{29}Si NMR results is beneficial for the further discussion. The span values (Ω) in Table 2 are between 80 and 85 ppm for ITQ-3 (ITE), Beta (*BEA), and ZSM-12 (MTW). The ^{19}F span value of [Cocp$_2$]-F-[Si−NON] (84.3 ppm) is also in this range.[28] These are the samples with ^{29}Si NMR signals between −140 and −150 ppm for the five-coordinate silicon units. The span values are considerably smaller for ITQ-4, Silicalite-1, and SSZ-23, which show the broad ^{29}Si NMR signals between −115 and −150 ppm. This observation indicates that dynamic motion of the fluoride ions exists in ITQ-4 and SSZ-23, as has been shown earlier for Silicalite-1.[15] Therefore, low-temperature ^{19}F and ^{29}Si NMR experiments have been performed in order to freeze out the motion of the fluoride ions. Low-temperature MAS NMR experiments are limited in time because of restrictions in keeping the low temperature and spinning of the sample stable for longer periods. Therefore, ^{29}Si MAS and ^{29}Si{^{19}F} CPMAS NMR experiments, which required typically 1 day of data acquisition at room temperature, were not performed at low temperatures.

(c) Low-Temperature ^{19}F MAS and ^{29}Si{^{1}H} CPMAS NMR. Figure 6 shows the ^{19}F MAS NMR spectra of MFI at various temperatures between 140 and 298 K. The spinning sideband distribution changes considerably with temperature, which means that the CSA varies with temperature. These changes are ascribed to the dynamic motion of fluoride ions which has been found by ^{29}Si NMR spectroscopy.[15] The study of anisotropic nuclear spin interactions, such as the CSA, is an excellent means of investigating motion.[29−31] A motional process reduces the chemical shift anisotropy to an extent that is a function of the mechanism and the time scale of the motion. At 140 K the fluoride motion is frozen out in MFI.[15] Interestingly, the span obtained by ^{19}F NMR, Ω, is 80.6 ppm at this temperature, a value that falls well within the range of what has been observed for the other zeolites at room temperature with no fluoride motion (Table 2). This value of 80.6 ppm is

(28) Wölker, A.; Koller, H.; Panz, C.; Behrens, C.; Villaescusa, L. A.; Camblor, M. A. 10th German Zeolite Conference, Bremen, March 9−11, 1998.

(29) Schmidt-Rohr, K.; Spiess, H. W. *Multidimensional Solid-State NMR and Polymers*; Academic Press: London, 1994.

(30) Wilhelm, M.; Firouzi, A.; Favre, D. E.; Bull, L. M.; Schaefer, D. J.; Chmelka, B. F. *J. Am. Chem. Soc.* **1995**, *117*, 2923.

(31) Koller, H.; Overweg, A. R.; Van de Ven, L. J. M.; De Haan, J. W.; Van Santen, R. A. *Microporous Mater.* **1997**, *11*, 9.
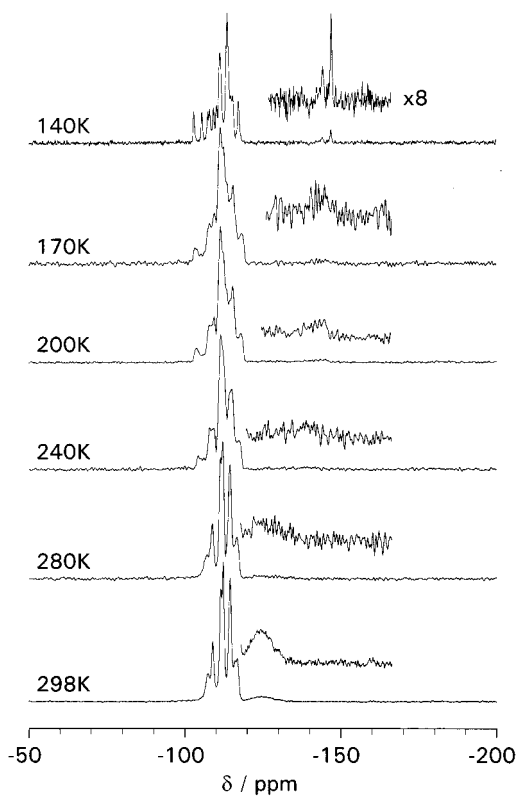

Figure 6. ^{19}F MAS NMR spectra of Silicalite-1 at various temperatures; the isotropic signal at 140 K is indicated by an arrow.

reduced at higher temperatures, and at 298 K a value of $\Omega = 52.3$ ppm is found. Thus, the motion is not isotropic at 298 K; otherwise the CSA would be completely averaged ($\Omega = 0$ ppm). Another interesting observation in Figure 6 is the change in the spinning sideband envelope between 240 and 280 K. In this temperature range the spinning sideband distribution changes from asymmetric (240 K) to nearly symmetric (280 K). The effect is expressed mainly by a discontinuity in the change of the asymmetry parameter, η, while the span, Ω, changes continuously over the whole temperature range. This change between 240 and 280 K is the most dramatic one over the entire temperature range in Figure 6, which means that the mechanism or time scale of the fluoride motion experiences the largest difference between 240 and 280 K.

The observations in the ^{19}F MAS NMR spectra of Figure 6 are confirmed by the ^{29}Si{^{1}H} CPMAS NMR spectra shown in Figure 7. At 140 K, where the fluoride motion is frozen out, two signals at −144.2 and −147.0 ppm are observed for the five-coordinate silicon sites, and the four-coordinate silicon has several lines between −103 and −118 ppm. We anticipate that the two signals for the SiO$_{4/2}$F$^-$ units are also due to J coupling, and not due to the presence of two sites. At 170 K all the signals get broader, especially those of the five-coordinate silicon, which broaden to an extent that makes them undetectable in the spectrum at 170 K in Figure 7. From 170 to 240 K the changes in the ^{29}Si{^{1}H} CPMAS NMR spectra are marginal, but a considerable change appears between 240 and 280 K. The number and the position of the signals of four-coordinate silicon change, and a very broad line is observed at ca. −130 ppm (280 K). The latter signal is due to an exchange between four- and five-coordinate silicon.[15] This observation of an event between 240 and 280 K is in good agreement with the changes observed in the ^{19}F MAS NMR spectra of Figure 6. This event between 240 and 280 K is interpreted by a change in the motion of fluoride ions. The observation that many signals are involved in the changes of the ^{29}Si{^{1}H} CPMAS NMR spectra at 240

Figure 7. $^{29}Si\{^1H\}$ CPMAS NMR spectra of Silicalite-1 (MFI) at various temperatures).

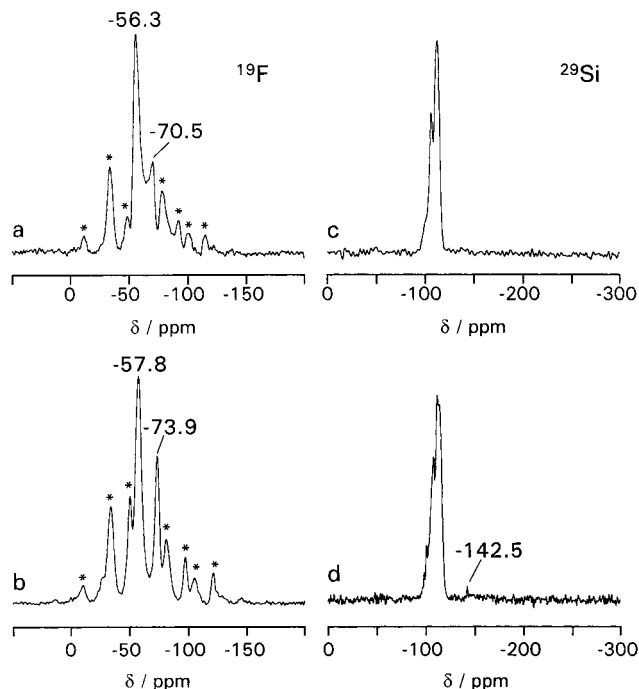**Figure 8.** ^{19}F MAS (a, b) and $^{29}Si\{^1H\}$ CPMAS (c, d) NMR spectra of SSZ-23 at 298 K (a, c) and at 140 K (b, d); spinning sidebands are marked by asterisks.

Table 3. ^{19}F Low-Temperature NMR Data of Zeolites ITQ-4 (IFR), Silicalite-1 (MFI), and SSZ-23 (STT)

	δ_{iso}/ ppm	δ_{11}/ ppm	δ_{22}/ ppm	δ_{33}/ ppm	Ω/ ppm	η	κ
ITQ-4 (130 K)	−71.3	−37.5	−57.9	−116.1	80.4	0.45	0.48
Silicalite-1 (140 K)	−69.9	−38.3	−52.6	−118.9	80.6	0.29	0.64
SSZ-23 (140 K)	−57.8	−22.5	−46.4	−104.5	80.0	0.51	0.42
	−74.0	−38.3	−52.9	−130.8	86.8	0.26	0.68

contrast, the spectrum at 140 K which is shown in Figure 8b has been simulated with two CSA components with Ω values of 80.0 and 86.8 ppm (Table 3), which is again an indication that the fluoride motion is frozen out at this temperature. Figure 8c and 8d show the $^{29}Si\{^1H\}$ CPMAS NMR spectra of SSZ-23 at 298 and 140 K, respectively. As shown above, the signal for five-coordinate silicon is very broad at room temperature, but the low-temperature experiment in Figure 8d clearly shows a sharp signal at −142.5 ppm for the $SiO_{4/2}F^-$ units in SSZ-23.

Low-temperature NMR experiments have also been performed on IFR, and, again, the span value in the ^{19}F CSA increases to the expected range (Ω = 80.4 ppm at 130 K). However, so far we have not succeeded to observe a ^{29}Si NMR signal of pentacoordinate silicon at low temperatures which is probably too broad. The ^{19}F CSA data of ITQ-4, Silicalite-1, and SSZ-23 at low temperatures are listed in Table 3.

4. Discussion

We have shown through ^{19}F and ^{29}Si solid-state NMR methods that there are Si−F interactions which seem to be rather common in the type of materials investigated. Depending on the specific phase and on the temperature, these interactions may correspond either to localized Si−F bonds (meaning that each F$^-$ ion binds to a specific Si atom and to that one only), or to reorienting bonds involving one fluorine and several silicon atoms in a dynamic situation. In several cases (MFI, STT, IFR) reorienting Si−F bonds are found at room temperature, but the fluoride motion is frozen out at low temperatures to give localized Si−F bonds. Earlier X-ray diffraction work on zeolites which now turn out to have localized Si−F bonds, based on the NMR results here, has shown that the fluoride ions are located in small cages with strong localized Si−F interactions.[1,11] The involved Si atoms are part of the zeolite framework, forming $SiO_{4/2}F^-$ units through sharing the four oxygen atoms with neighboring tetracoordinated $SiO_{4/2}$ units.

Actually, it was common in early reports on the fluoride route to conclude that occluded fluoride ions formed ion pairs with the organic cation within the zeolite channels.[18a] However, more recent structural work using X-ray diffraction suggests that this is not the case. So far the location of F$^-$ in five high-silica phases has been proposed (Table 4), based upon single crystal or powder diffraction experiments. In the case of MFI two contradictory reports located fluoride ions either in the main channel[18a] or in a small interstice[18b] of the SiO_2 framework. Our NMR experiments strongly suggest a close distance between fluoride and silicon in MFI; thus the location of fluoride in the main channel (shortest Si−F distance 4.19 Å) can be discredited. It is very interesting that F$^-$ has always been found inside small cages of the SiO_2 framework (Table 4), and that the shortest Si−F distances are in the range from 1.8 to 2.6 Å. Interestingly, there is a trend observed between the shortest Si−F distances (Table 4) and the ^{19}F chemical shifts and span values (Tables 2 and 3). If the Si−F distance increases, the chemical shift is at lower field and the span value decreases. However, more data points would be needed to confirm this trend, and it will

and 280 K in Figure 7 suggests that the mechanism of the fluoride motion is complicated, probably involving more than two framework silicon sites.

Another example with fluoride motion, SSZ-23, is shown in Figure 8. The ^{19}F MAS NMR spinning sideband spectrum of Figure 8a shows two components. However, the sideband intensities could not be simulated with an appropriate CSA model which is consistent for two different magnetic fields. By

Table 4. Proposed Locations of Fluoride in As-made Silica Zeolites

phase	X-ray diffraction data	fluoride location[a]	$d(Si-F)^{b}/$ Å
[Cocp$_2$]-F-[Si-NON]	single crystal (220 K) [ref 1]	[$4^1 5^4 6^2$] cage	1.836
[Q]-F-[Si-AST]	single crystal [ref 19]	[4^6] cage	2.633
[BQ]-F-[Si-IFR]	powder (synchrotron) [ref 10]	[$4^3 5^2 6^1$] cage	2.21
[TMAda]-F-[Si-STT][c]	single crystal (synchrotron 160K) [ref 11]	[$4^3 5^4$] cage	1.94 1.95 1.96
[TPA]-F-[Si-MFI]	powder [ref 18b]	[$4^1 5^2 6^2$] cage	2.20 2.56
	twinned crystal [ref 18a]	channel inter-sections	≥4.19

[a] Cages denoted as [$n'^{m'} n''^{m''}$...] according to the number m of windows with n Si atoms surrounding the cage. [b] When there is not a clear Si−F bond (i.e., when the Si−F distance is larger than 2 Å), only Si−F distances smaller than the sum of the van der Waals radius of F and the nonbonded radius of Si[37] (1.35+1.53 = 2.88 Å) were considered. [c] At 160 K, three close fluoride locations with partial occupancies were proposed.

be interesting in future work to explore the reason for this interesting observation.

The fluoride route to the hydrothermal synthesis of zeolites has been known for the last 20 years. However, relatively little understanding of this kind of chemical system has been gained, despite the wealth of microporous silica phases obtained.[7−11] This synthetic route is intriguing in several aspects, notably in that it appears to be very well suited for the synthesis of pure and high silica phases, including catalytically active materials containing Al or Ti in framework positions. Another worthy characteristic of the method is the high degree of perfection of the silica network obtained after calcination, which may be attributed to the low concentration of connectivity defects. This perfection refers to both long-range and short-range order, and affords the opportunity to obtain a high resolution of peaks in several characterization techniques, thus giving new opportunities for the understanding of this kind of materials. For example, the high degree of perfection of ITQ-4 allowed its crystal structure to be solved from powder synchrotron X-ray diffraction experiments through direct methods,[10] and the locations of the relatively disordered SDA cation and the fluorine anion could also be found.[32] On the other side, the short-range order of the calcined samples translates into a very high resolution of crystallographic sites in the ^{29}Si MAS NMR spectrum, which in turn may be used to obtain structural information (such as average Si−O−Si angles for each resolved site).[33] This is in contrast with the poor resolution obtained for silica samples prepared by the hydroxide route. An enhanced resolution of the infrared spectrum in the range of framework vibrations is also apparent for the calcined zeolites that have been made by the fluoride method.[34]

Thus, a crucial aspect of the fluoride route is why the obtained phases present few connectivity defects. Occlusion of F$^-$ is probably the main reason for this effect, since it affords charge balance of the SDA without recourse to Si−O$^-$ defects, and also avoids the stabilization of additional Si−OH defects as the extensive formation of strong Si−O$^-$···HO−Si bonds is now prevented.

Scheme 3
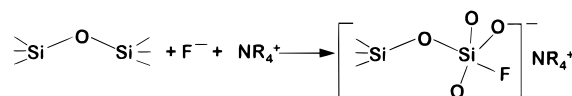
The results presented in this work may also have strong implications on other aspects of the synthesis of zeolites by the fluoride route, and specifically on the phase selectivity issue, which is a main problem in the synthesis of zeolites and in the desired goal of a priori designing new zeolite phases. We have recently demonstrated the feasibility of synthesizing pure silica frameworks of very low density through the fluoride route without recourse to new and highly specific structure-directing agents.[35] The results presented here suggest a ubiquitous interaction between F and Si in silica phases. We have demonstrated the strong chemical affinity of F$^-$ for silicon, even when this is already four-coordinated to oxygen in a SiO$_2$ network. This in turn poses the question of whether the interaction of F$^-$ with nearby framework silicon atoms may provide an additional stabilization of the SiO$_2$/SDA/F host/guest compound. At room temperature such an interaction of F$^-$ with the framework may be localized or dynamically disordered, involving several Si atoms, and it is possibly highly disordered at the synthesis temperatures (typically above 373 K). Thus, future investigations, especially quantum mechanical calculations on the stability of silica phases under the synthesis conditions in the presence of fluoride, should take into account the results presented here.

5. Conclusions

The positive charge of organic structure-directing agents in high-silica zeolites that are synthesized in fluoride medium are in general balanced by SiO$_{4/2}$F$^-$ units in the zeolite framework. The nucleophilic addition of F$^-$ ions at the SiO$_2$ framework can be expressed by the formal equation (Scheme 3) which indicates a structural integration of the charge-balancing species different from the case with OH$^-$ (see above). In some zeolites (MFI, IFR, SSZ-23) the fluoride ions exchange in a dynamic process between different framework silicon sites at room temperature. This motion is frozen out at low temperatures (130−140 K).

The ^{29}Si chemical shifts of five-coordinate silicon units without fluoride motion are between −140 and −150 ppm. When the fluoride ions exchange between several framework silicon sites, a broad averaged ^{29}Si NMR signal is observed between −115 and −150 ppm. The isotropic ^{19}F chemical shifts do not provide any indication whether there is motion. However, the chemical shift anisotropy, especially the span value, Ω, turns out to be a useful parameter to distinguish between fluoride ions with and without dynamic motion. Ω is between 80 and 87 ppm if the fluorine is rigidly bound to the zeolite framework, forming SiO$_{4/2}$F$^-$ units. The value of Ω is reduced in the case of motion which is due to tensor averaging, and the extent of the reduction is a function of the mechanism and time scale of the motion.[29] When the motion of the fluoride ions is frozen out at low temperatures, then the span, Ω, has a value which is typical of zeolites without fluoride motion.

(32) Barrett, P. A.; Camblor, M. A.; Corma, A.; Jones, R. H.; Villaescusa, L. A. *J. Phys. Chem. B* **1998**, *102*, 4147.

(33) Engelhardt, G.; Michel, D. *High-Resolution Solid-State NMR of Silicates and Zeolites*; Wiley: Chichester, 1987.

(34) Camblor, M. A.; Corma, A.; Valencia, S. *J. Mater. Chem.* **1998**, *8*, 2137.

(35) Barret, P. A.; Camblor, M. A.; Corma, A.; Díaz-Cabañas, M. J.; Valencia, S.; Villaescusa, L. A. 12th International Zeolite Conference, Baltimore, MD, July 5−10, 1998.

(36) Patarin, J.; Soulard, M.; Kessler, H.; Guth, J.-L.; Baron, J. *Zeolites* **1989**, *9*, 397.

(37) O'Keeffe, M.; Hyde, B. G. in "Structure and Bonding in Crystals", O'Keefe, M., Navrotsky, A., Eds.; Academic Press, New York, 1981, pp 227−254.

JA9840549